

Article

Cyclic Performance of Structural Steels after Exposure to Various Heating–Cooling Treatments

Peng Du ¹, Hongbo Liu ^{1,2,3,*} and Xuchen Xu ^{2,3}¹ School of Civil Engineering, Hebei University of Engineering, Handan 056038, China; dupeng@hebeu.edu.cn² State Key Laboratory of Hydraulic Engineering Simulation and Safety, Tianjin University, Tianjin 300072, China; xcxu@tju.edu.cn³ School of Civil Engineering, Tianjin University, Tianjin 300072, China

* Correspondence: hbliu@tju.edu.cn

Abstract: The cyclic performance of structural steels after exposure to various elevated temperatures and cooling-down methods was experimentally investigated in this paper. Four types of frequently used structural steels were tested including Chinese mild steel Grade Q235, Chinese high-strength steel Grade Q345, and Chinese stainless steel Grade S304 and S316. A total of eighty specimens were prepared using three different heating–cooling processes before being subjected to cyclic loads. The post-fire basic features and hysteretic performances of the four types of structural steels exposed to various target temperatures (100–1000 °C), heat soak times (30 min or 180 min) and cooling-down methods (natural air or water) were recorded and discussed. The results show that all the tested structural steels prepared using different heating–cooling treatments exhibited proper ductility and energy dissipation capacity, while the heat soak times and cooling-down methods had a definite effect on their energy dissipation capacity; no Masing phenomenon was found in the tested structural steels. Finally, a set of skeleton curves were proposed for the four types of structural steels under cyclic loading based on the Ramberg–Osgood model, which could serve as the foundation for the seismic capacity evaluation of steel structures after a fire.



Citation: Du, P.; Liu, H.; Xu, X. Cyclic Performance of Structural Steels after Exposure to Various Heating–Cooling Treatments. *Metals* **2022**, *12*, 1146.

<https://doi.org/10.3390/met12071146>

Academic Editors: Andrey Belyakov and Ulrich Prael

Received: 9 May 2022

Accepted: 26 June 2022

Published: 5 July 2022

Publisher's Note: MDPI stays neutral with regard to jurisdictional claims in published maps and institutional affiliations.



Copyright: © 2022 by the authors. Licensee MDPI, Basel, Switzerland. This article is an open access article distributed under the terms and conditions of the Creative Commons Attribution (CC BY) license (<https://creativecommons.org/licenses/by/4.0/>).

Keywords: structural steel; elevated temperatures; cooling-down method; cyclic performance; skeleton curve

1. Introduction

Structural steels have become one of the most widely used materials in civil engineering owing to their light weight, high strength, excellent ductility, and good energy dissipation capacity. However, it has been demonstrated that the mechanical properties of structural steels are changed in a fire. Therefore, the performance of structural steels after exposure to elevated temperatures is important for the post-fire reliability evaluation of steel structures.

Extensive studies were conducted on the post-fire mechanical properties of structural steels, which found that the post-fire mechanical properties of structural steels are dependent on steel grades, cold forming procedures, exposure temperatures, heating methods, and cooling methods [1,2]. Corresponding predictive equations for the mechanical properties of structural steels were proposed to incorporate the aforementioned factors into those studies.

The post-fire mechanical properties of high-strength steels were found to be quite different from those of mild steels [3,4]. For Chinese hot-rolled Q235, Q345, and Q420 steels and ASTM A572 Gr.50 steels, their post-fire mechanical properties changed significantly after exposure to temperatures above approximately 700 °C [1,5]. The post-fire mechanical properties of European standard high-strength steels, including S460, S690, and S960, are not obviously affected until the temperature reaches above 600 °C, and they begin to degrade after cooling down from the temperatures beyond 600 °C up to 1000 °C [3,6,7].

Furthermore, the critical temperatures turn into approximately 400 °C–700 °C for the Chinese high-strength steels Grade Q460 and Q690 when cooled by air, water, and fire-fighting foam [4,8–12]. For cold-formed steels, the post-fire mechanical properties are reduced after they have been exposed to temperatures exceeding 300 °C [1,13].

The heating rate and repeated heating/cooling were found to affect the post-fire elastic modulus and yield strength of high-strength steel Q690; however, the effect on tensile strength and fracture strain was negligible [9]. Conversely, no obvious effect of cyclic heating–cooling was observed in hot-rolled Q235, Q345, Q420, and cold-formed Q235 steel [1]. Due to the microstructure transformation, the cooling method has been found to have an obvious influence on the residual strength and ductility of structural steel after exposure to sufficiently elevated temperatures, whereas there is no observable influence on elastic modulus [1,8–10]. The strength enhancement of structural steels due to cold forming or heat treatment is weakened with increasing heat treatment target temperatures, but their ductility is observed to be recovered [1,7,14]. Stainless steels show superior post-fire performance and a higher strength retention capacity than carbon steels [14–16]. According to some studies [17,18], the heat soak time was found to have a negligible effect on the post-fire mechanical properties of carbon steels and austenitic stainless steels, whereas other studies have shown that the ductility of lean duplex stainless steels and high-strength quenched and tempered steels are improved with heat soak time [16,19].

Most spatial structures can avoid collapse after a fire event, owing to their sufficient redundancy. For economic reasons, these fire-suffered spatial structures are considered to remain in service after a post-fire reliability evaluation. The post-fire seismic capacity is one of the most important components in the post-fire reliability evaluation. The mechanical properties of structural steels under cyclic loading are quite different from those under monotonic loading, and the hysteretic properties of structural steels play a pivotal role in the seismic performance of structures [20,21]. According to the review of state-of-the-art literature, most of the included studies focused on the post-fire mechanical properties of structural steels under monotonic loading conditions, and the post-fire cyclic performance of structural steels was rarely discussed. This paper therefore presents a detailed experimental study on the post-fire mechanical properties of commonly used structural steels under cyclic loading condition, including Chinese mild steel Grade Q235, Chinese high-strength steel Grade Q345, and Chinese stainless steel Grade S304 and S316. There were three heating–cooling treatments considered in the preparation of the specimens. Research funding can serve as the foundation for the seismic capacity evaluation of steel structures after a fire.

2. Experimental Programs

2.1. Specimen Design

Chinese mild steel Grade Q235, Chinese high-strength steel Grade Q345, and Chinese stainless steel Grade S304 and S316 were tested in this paper, and were in accordance with GB/T700-2006, GB/T1591-2008, GB/T1220-2007, and GB/T3280-2015, respectively [22–25]. According to GB/T 15248-2008 [26], eighty-four specimens were designed and classified into four groups according to their steel categories. Each specimen group had twenty-one specimens and each included one room-temperature specimen and twenty heating–cooling-treated specimens exposed to different heating treatments and cooling-down methods. Figure 1a,b show the dimensions of specimens for Q235/Q345 and S304/S316, respectively.

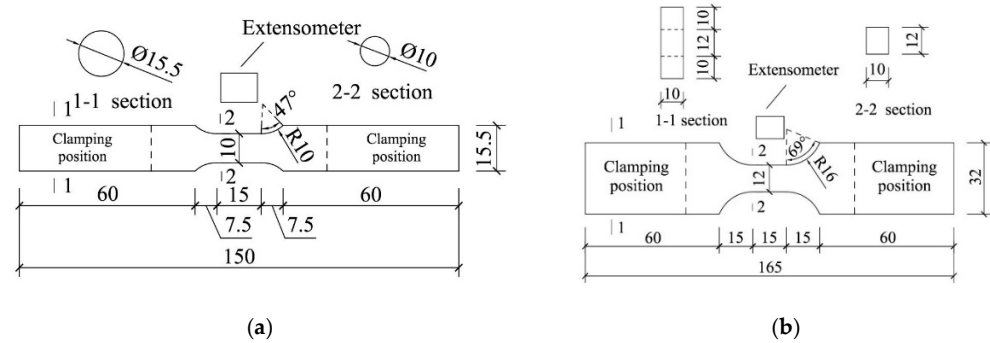


Figure 1. Dimensions of specimens. (a) Q235 and Q345; (b) S304 and S316.

2.2. Experiment Procedure

There were two stages during the whole experiment procedure. In the first stage, the specimens were heated to the preselected elevated temperatures and cooled down to room temperature according to three different heating–cooling treatments. In the second stage, the prepared specimens were tested under cyclic loading at room temperature.

2.2.1. Heating–Cooling Treatment

As shown in Figure 2, three heating–cooling treatment styles, with each including four stages per style, were employed in the preparation of specimens, which were marked as style 1, style 2, and style 3, respectively. In the three heat treatment styles, all the specimens were first heated at a rate of 20 °C/min to a temperature of 50 °C less than the target temperature with a temperature-controlled electric furnace SX-G36123 (Tianjin Zhonghuan Furnace Corporation, Tianjin, China). This temperature was maintained for 15 min before the next step. Then, the specimens were continually heated at a rate of 5 °C/min to a temperature of 10–15 °C less than the target temperature, and the temperature was maintained for 10 min at this time. Subsequently, the specimens were heated at a rate of 5 °C/min to the target temperature, and the heat soak times at the target temperature were 30 min, 180 min, and 30 min for heat treatment process styles 1–3, respectively. The heat processes described above were to ensure a uniform temperature distribution in the specimens. For heat treatment process style 1, ten elevated target temperatures were set, i.e., 100 °C, 200 °C, 300 °C, 400 °C, 500 °C, 600 °C, 700 °C, 800 °C, 900 °C, and 1000 °C. As a contrast, five elevated target temperatures were selected for heat treatment process styles 2 and 3, respectively, i.e., 100 °C, 300 °C, 500 °C, 700 °C, and 900 °C. After the specified heat soak times, the specimens were allowed to cool down to room temperature. A natural air cooling method was used in the heat treatment process styles 1 and 2, and a water cooling method was applied in heat treatment process style 3. Figure 3a,b show the prepared specimens.

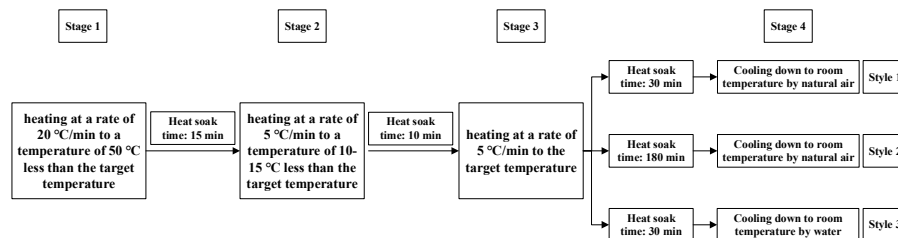


Figure 2. Heating–cooling treatment process.

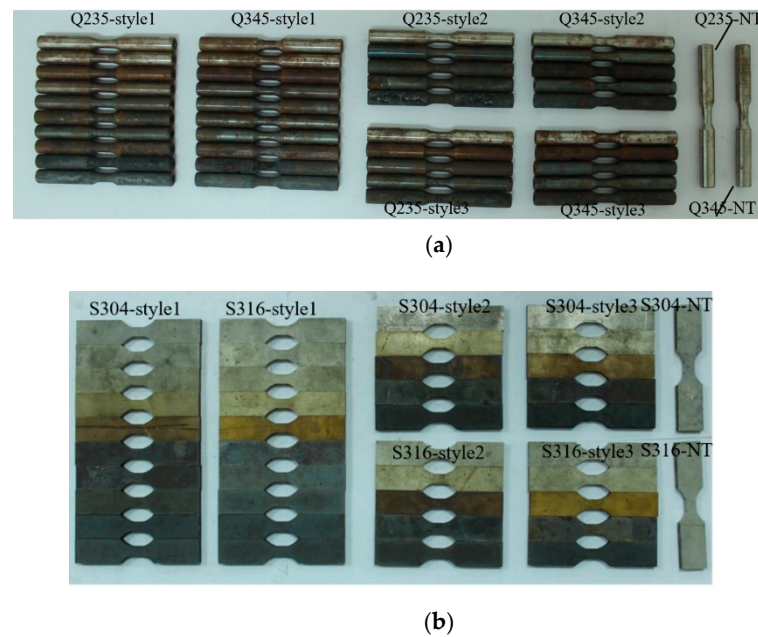


Figure 3. Prepared specimens. (a) Q235 and Q345; (b) S304 and S316.

2.2.2. Cyclic Test

The cyclic loads and monotonic loads were applied to the prepared specimens using the fatigue-testing machine Instron 8801 (Instron Corporation, Norwood, MA, USA). The applied loads were also recorded with the machine at the same time. A 5 mm range extensometer with a 12.5 mm gauge length was selected to measure the strain on the specimens.

The cyclic loading processes were controlled by strain at a rate of 0.0005/s, and the cyclic loading protocol was different for Q235/Q345 specimens and S304/S316 specimens, as shown in Figure 4a,b. After the specified loading cycles, the specimens were monotonically loaded till failure at a strain rate of 2 mm/min.

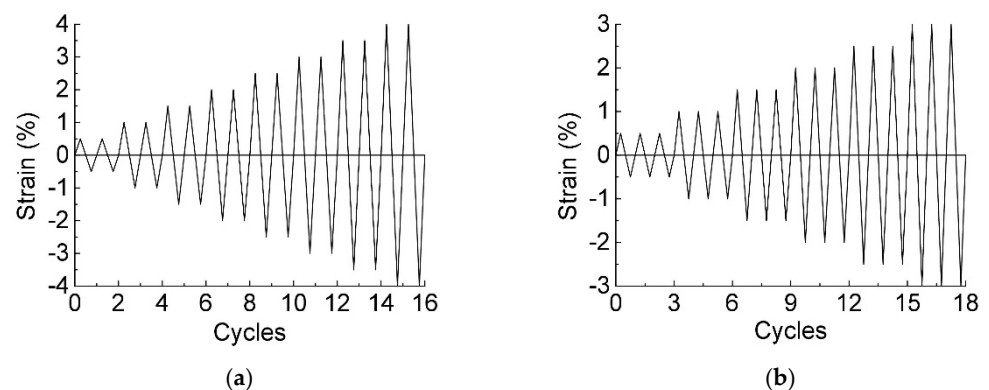


Figure 4. Loading protocol. (a) Q235 and Q345; (b) S304 and S316.

3. Experimental Results and Discussion

3.1. Post-Fire Basic Features of Structural Steels

The first tensile stage in the first loading cycle of the hysteretic curve was extracted for each specimen to evaluate the initial elastic modulus E_s and the initial yielding strength f_y (nominal yielding strength for stainless steels) of the tested structural steels, as shown in Figure 5a,b. The ultimate strength f_u and fracture strength f_{u1} of each specimen after cyclic loading was analyzed using the monotonic loading process mentioned in Section 2.2.2, as shown in Figure 5c,d. To study the effect of heating–cooling treatments on the basic

features of structural steels, the residual factors (R) were calculated and discussed based on the data from Figure 5 in Sections 3.1.1–3.1.3, which were defined as the ratio of the mechanical properties after cooling down from various elevated temperatures to that at room temperature without fire exposure.

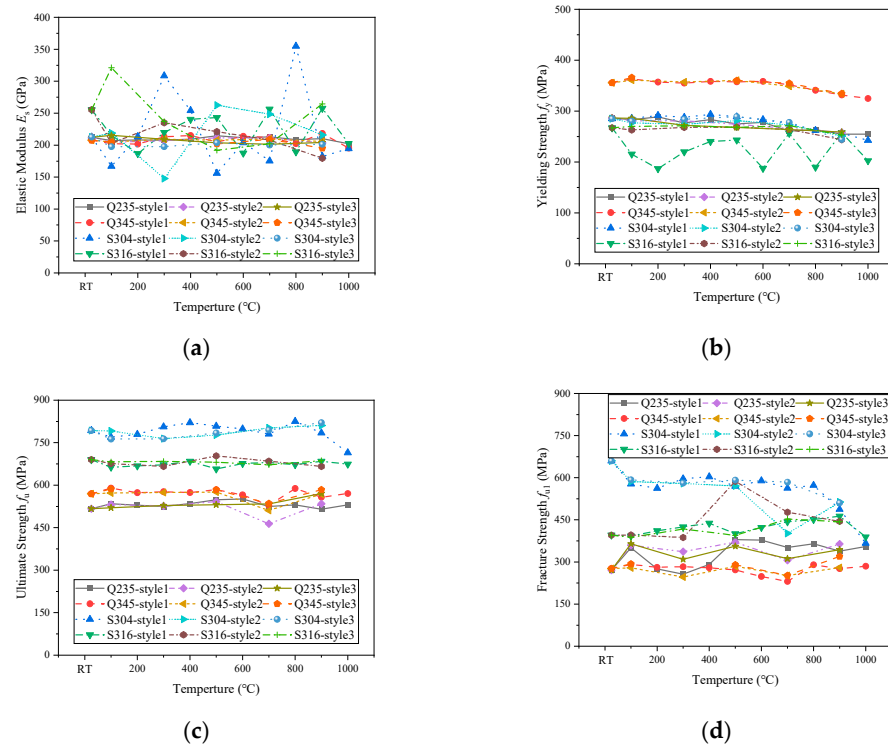


Figure 5. Basic features of structural steels. (a) Elastic modulus; (b) Yielding strength; (c) Ultimate strength; (d) Fracture strength.

3.1.1. Elastic Modulus

The post-fire elastic moduli (E_s) of the tested structural steels were calculated according to GB/T 22315-2008 [27]. Figure 6a,b show the elastic modulus residual factor (R_E) for all four types of structural steels. The Q235, Q345, and S304 steel specimens maintained their initial elastic moduli after exposure to temperatures up to 1000 °C and cooling down using different methods, with fluctuation being less than $\pm 10\%$. By contrast, a 10–20% decrease in elastic moduli was found in the S316 steel specimens when treated with heating–cooling treatment styles 1 and 2. For the S316 steel specimens prepared with heating–cooling treatment style 3, the measured elastic modulus was initially increased by about 25% after exposure to 100 °C, and then it was dropped dramatically by about 10%, 25%, and 20% after exposure to 300 °C, 500 °C, and 700 °C, respectively. Moreover, the elastic modulus of the S316 steel specimen after exposure to 900 °C and cooling down by water regained its initial elastic modulus. The post-fire elastic moduli of the studied specimens indicated that the effect of target heat temperatures, heat soak times, and cooling-down methods on the elastic moduli of Q235, Q345, and S304 steels after exposure to elevated temperatures up to 1000 °C (900 °C for heating–cooling treatment styles 2 and 3) was negligible, while the influence of elevated temperatures and cooling-down methods on the elastic moduli of S316 steels was significant.

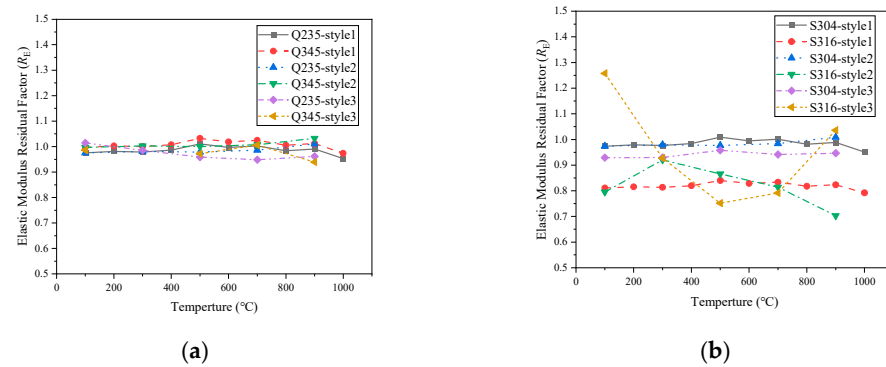


Figure 6. Elastic modulus residual factor. (a) Q235 and Q345; (b) S304 and S316.

3.1.2. Yielding Strength

The post-fire yielding strength (nominal yielding strength for stainless steels) residual factors (R_{fy}) are illustrated in Figure 7. No obvious change was found in the yielding strength of all four types of structural steels until the temperature reached 700 $^{\circ}\text{C}$, after which the post-fire yielding strength of Q235 and Q345 steels was decreased slightly, and a reduction of about 10% was observed after exposure to 1000 $^{\circ}\text{C}$ (900 $^{\circ}\text{C}$ for heating–cooling treatment styles 2 and 3), as shown in Figure 7a. A decrease at a relatively rapid rate was found in the yielding strength of S304 and S316 steels after exposure to temperatures exceeding 700 $^{\circ}\text{C}$, and reductions of approximately 15% were observed when the exposure temperature reached 1000 $^{\circ}\text{C}$ (900 $^{\circ}\text{C}$ for heating–cooling treatment styles 2 and 3), as shown in Figure 7b. The results showed that the critical temperature of yielding strength was about 700 $^{\circ}\text{C}$ for all four types of structural steels. The influences of different cooling methods on the residual yielding strength of the studied structural steels were insignificant in this experiment.

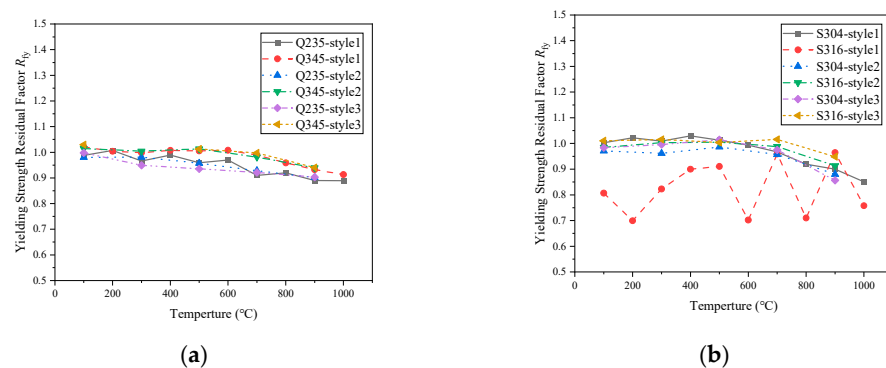


Figure 7. Yielding strength residual factor. (a) Q235 and Q345; (b) S304 and S316.

3.1.3. Ultimate Strength

The ultimate strength residual factors (R_{fu}) of the tested specimens are described in Figure 8a,b. The ultimate strength of all four types of structural steels experienced a fluctuation within a narrow range, and the maximum magnitude of the changes was within 10%. This phenomenon implied that the heating–cooling treatment styles discussed in this paper may have limited effects on the ultimate strength of all four types of structural steels after cyclic loading.

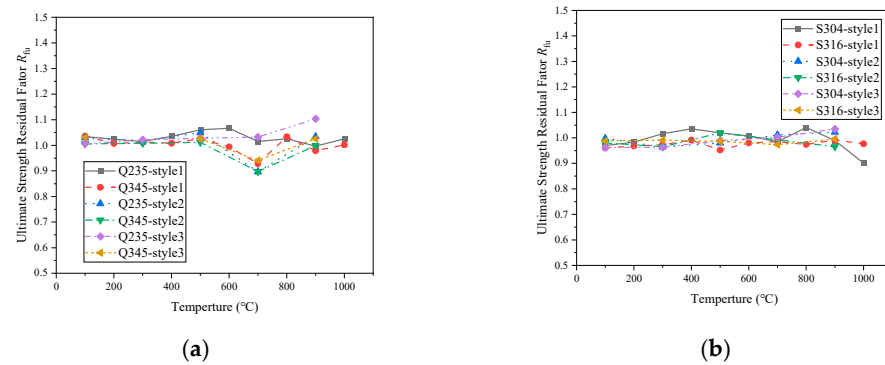


Figure 8. Ultimate strength residual factor. (a) Q235 and Q345; (b) S304 and S316.

3.1.4. Fracture Strength

The post-fire fracture strengths of all four types of structural steels were decreased compared to their corresponding ultimate strengths without fire influence, and the fracture strength drop ratios (D_{fu1}) were defined as $(f_u - f_{u1})/f_u$, as shown in Figure 9a,b. It can be found that all the fracture strength drop ratios were larger than 15%, which is the limit of the seismic design requirements [11]. This meant that the tested structural steels still exhibited good seismic ductility after exposure to heating–cooling processes. Moreover, the influence of steel grades on the fracture strength drop ratios was more significant than the target temperatures and cooling-down methods of heating–cooling treatments discussed in this paper.

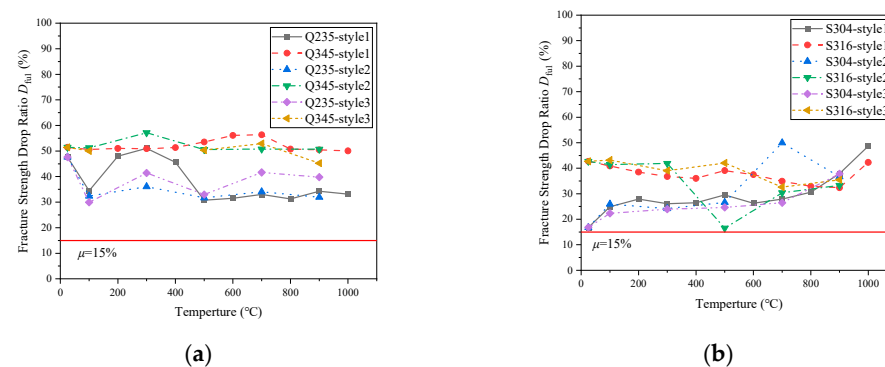


Figure 9. Fracture strength drop ratio. (a) Q235 and Q345; (b) S304 and S316.

3.2. Post-Fire hysteretic Performance of Structural Steels

3.2.1. Hysteretic Curve

In this section, the specimens exposure to room temperature are marked as S-NT, and other specimens are coded as shown in Figure 10. The hysteretic strain–stress curves of the tested specimens are shown in Figures 11–14, and subfigures (a–j) in each figure show the data at different elevated target temperatures.

All the tested specimens had plump hysteretic curves, which meant no buckling failure appeared in the specimens, which was in accordance with the failure modes observed during the experiment. Moreover, no obvious degradation of strength and stiffness was found in the hysteretic curves for the same strain levels. Therefore, all four types of structural steels had good ductility under cyclic loading despite the heating–cooling cycle they experienced.

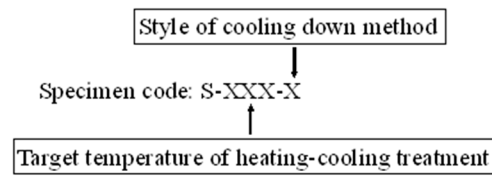


Figure 10. Specimen code.

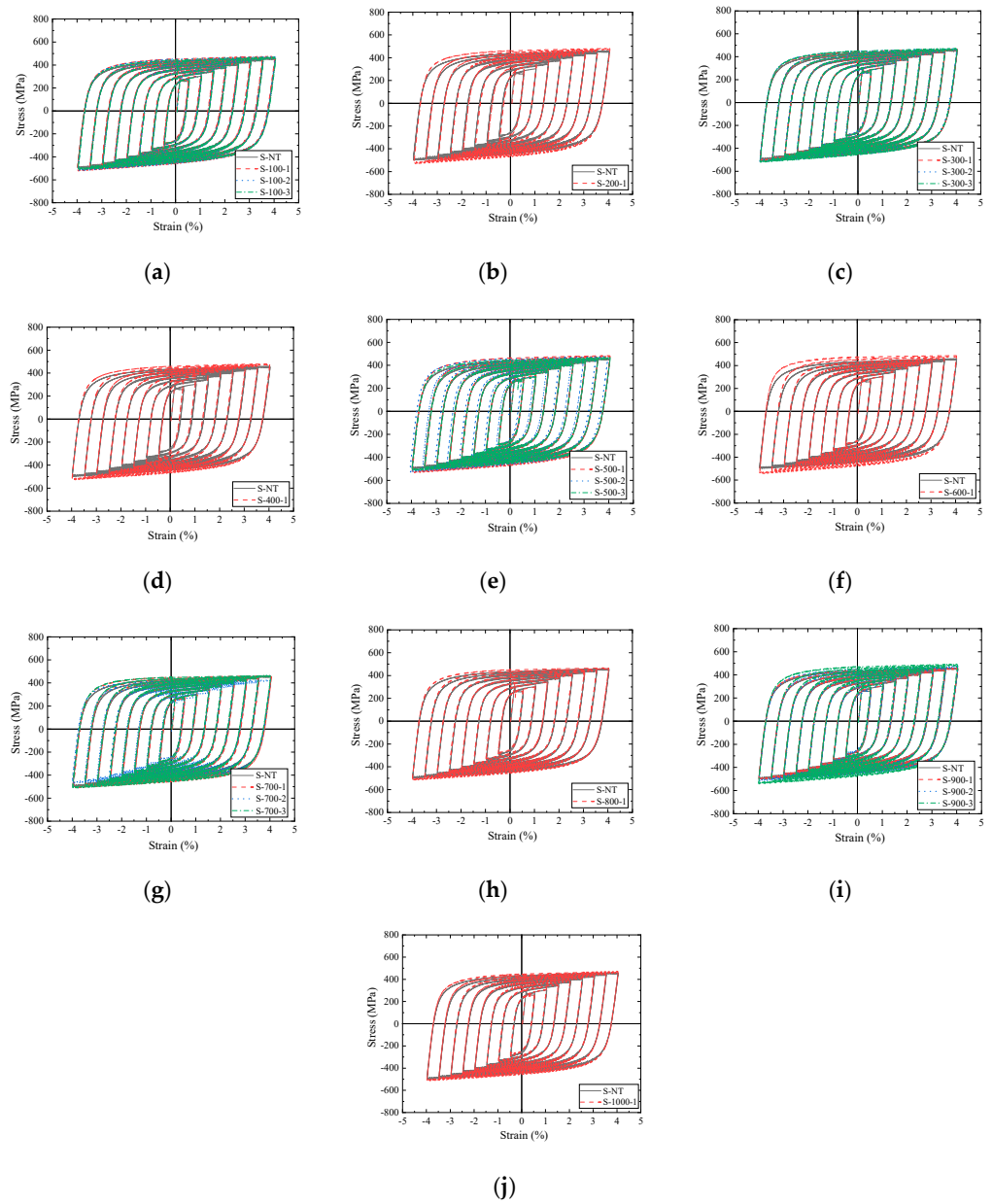


Figure 11. Hysteretic curves of Q235. (a) 100 °C; (b) 200 °C; (c) 300 °C; (d) 400 °C; (e) 500 °C; (f) 600 °C; (g) 700 °C; (h) 800 °C; (i) 900 °C; (j) 1000 °C.

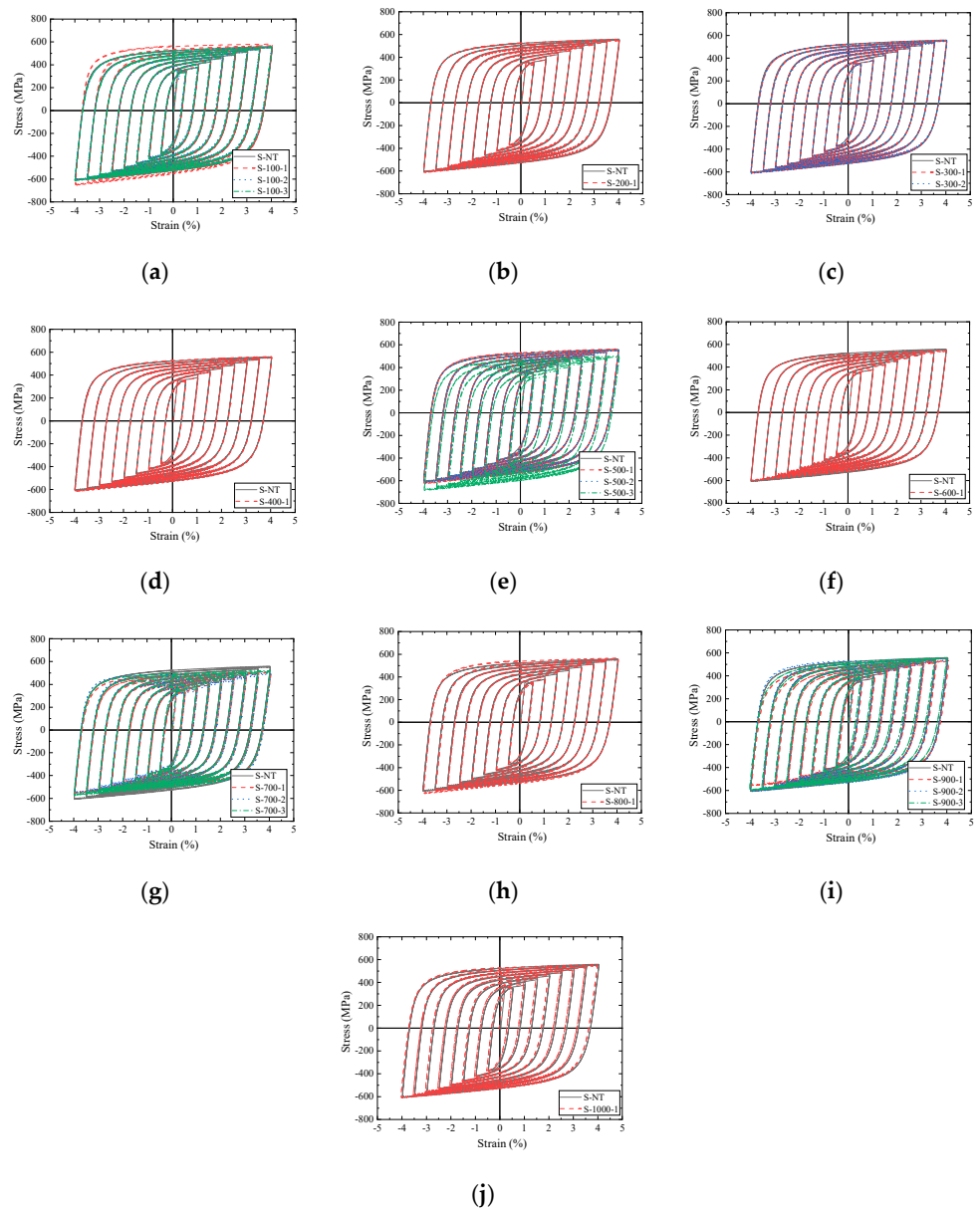


Figure 12. Hysteretic curves of Q345. (a) 100 °C; (b) 200 °C; (c) 300 °C; (d) 400 °C; (e) 500 °C; (f) 600 °C; (g) 700 °C; (h) 800 °C; (i) 900 °C; (j) 1000 °C.

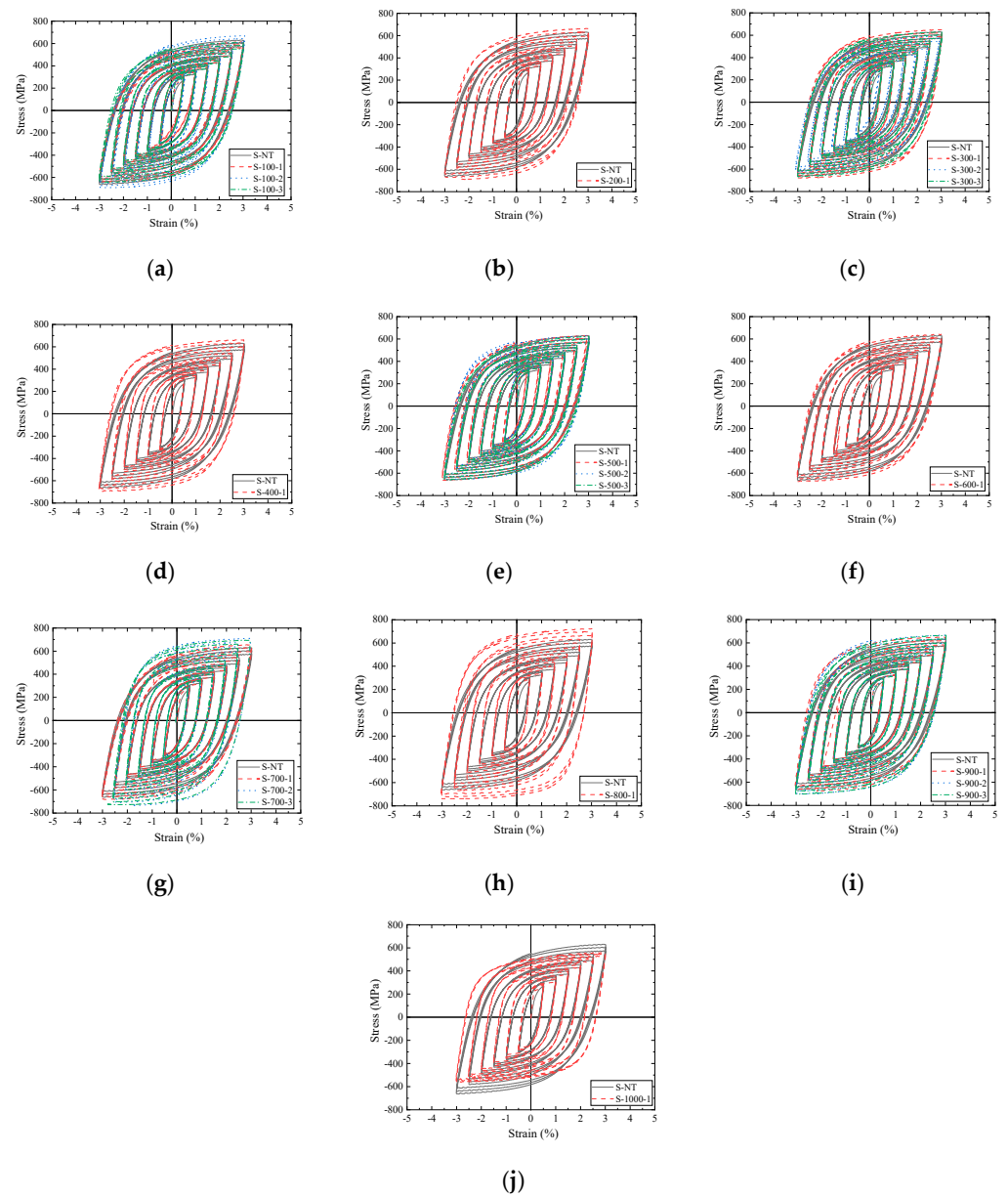


Figure 13. Hysteretic curves of S304. (a) 100 °C; (b) 200 °C; (c) 300 °C; (d) 400 °C; (e) 500 °C; (f) 600 °C; (g) 700 °C; (h) 800 °C; (i) 900 °C; (j) 1000 °C.

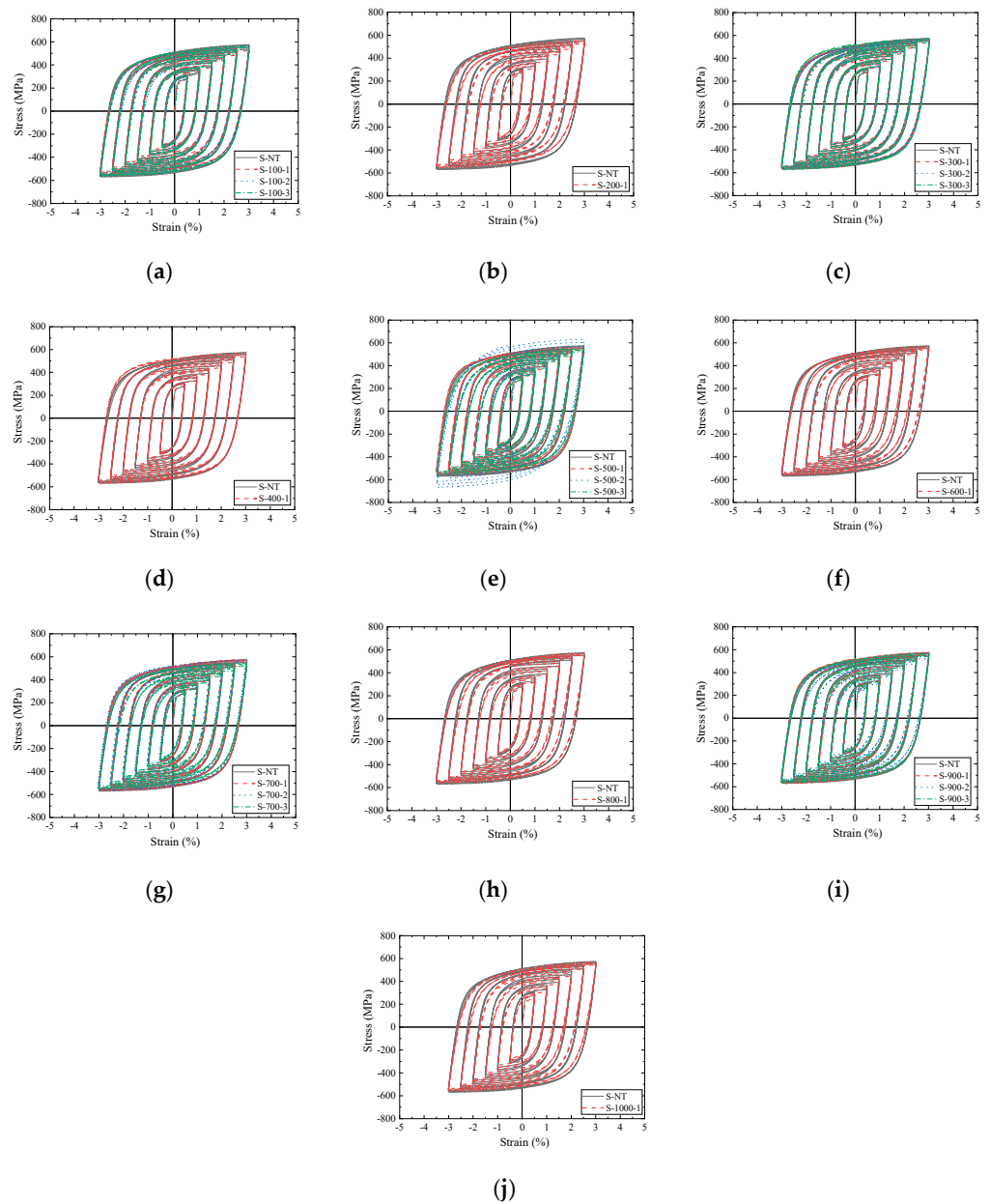


Figure 14. Hysteretic curves of S316. (a) 100 °C; (b) 200 °C; (c) 300 °C; (d) 400 °C; (e) 500 °C; (f) 600 °C; (g) 700 °C; (h) 800 °C; (i) 900 °C; (j) 1000 °C.

3.2.2. Masing Property

If the hysteresis loops of the metal obtained at different strain ranges coincide when they are plotted in relative coordinates, it means that the metal has a “Masing” property and the yield characteristics are the same [28]. To study the “Masing” properties of the tested structural steels in this paper, the hysteresis curves obtained in the last Section were reproduced as relative hysteretic curves in the relative coordinate system in this Section, and the relative hysteretic curves of typical specimens (room temperature, 900 °C) are shown in Figures 15–18 [29,30], and subfigures (a–d) show the relative hysteretic curves of the specimens prepared by different heating-cooling treatments.

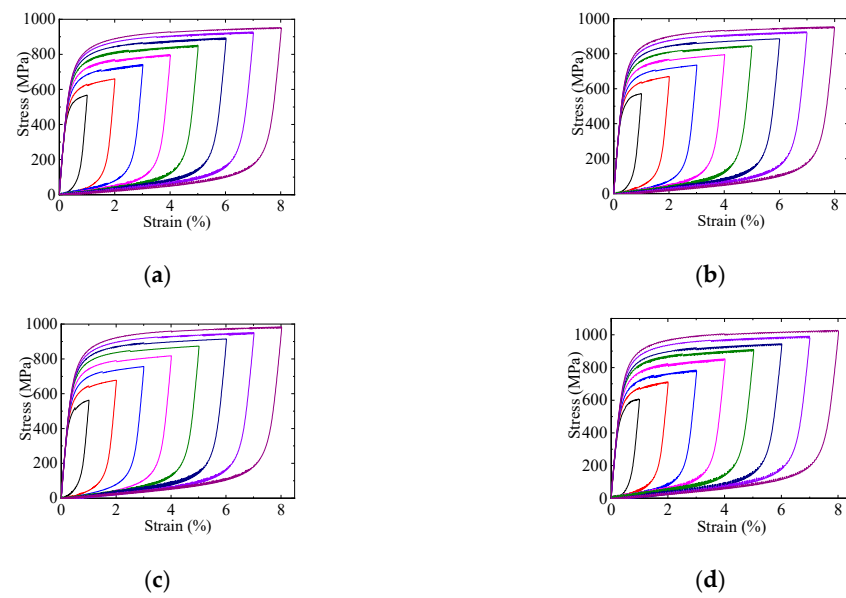


Figure 15. Relative hysteretic curves of Q235. (a) S-NT; (b) S-900-1; (c) S-900-2; (d) S-900-3.

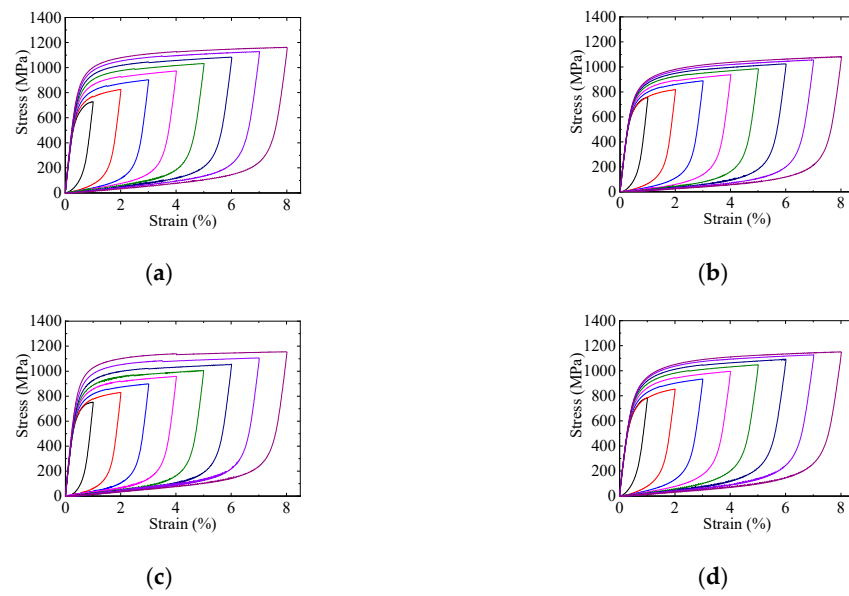


Figure 16. Relative hysteretic curves of Q345. (a) S-NT; (b) S-900-1; (c) S-900-2; (d) S-900-3.

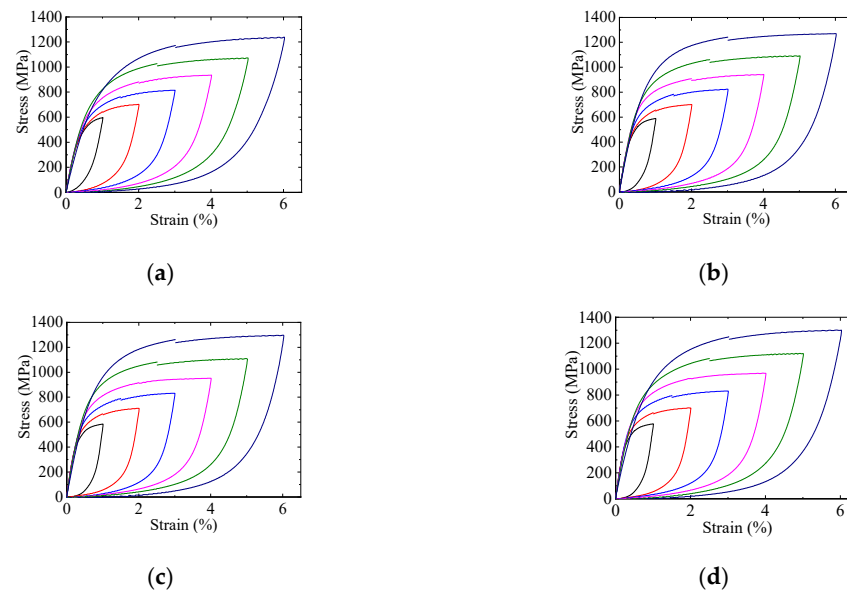


Figure 17. Relative hysteretic curves of S304. (a) S-NT; (b) S-900-1; (c) S-900-2; (d) S-900-3.

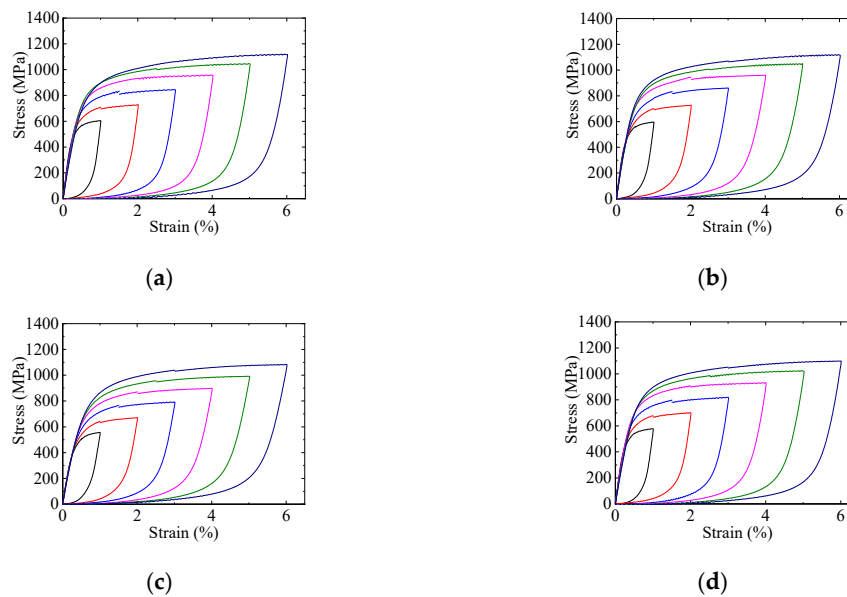


Figure 18. Relative hysteretic curves of S316. (a) S-NT; (b) S-900-1; (c) S-900-2; (d) S-900-3.

As indicated in Figures 15–18, the relative hysteretic curves obtained at different strain levels did not coincide with each other, which revealed that the four types of structural steels tested in this paper had non-Masing properties, which was unrelated to target heat temperatures, heat soak times, and cooling-down methods.

3.2.3. Energy Dissipation Capacity

Structural steels can dissipate energy when they experience plastic deformations, which can be measured as the area of hysteretic loops. The second loop at each strain level was extracted from the hysteretic curves of all four types of structural steel specimens and used to calculate the area of the hysteretic loops and evaluate their energy dissipation capacity. To save space, typical heat target temperatures were selected during the energy dissipation capacity evaluation, as shown in Figure 19.

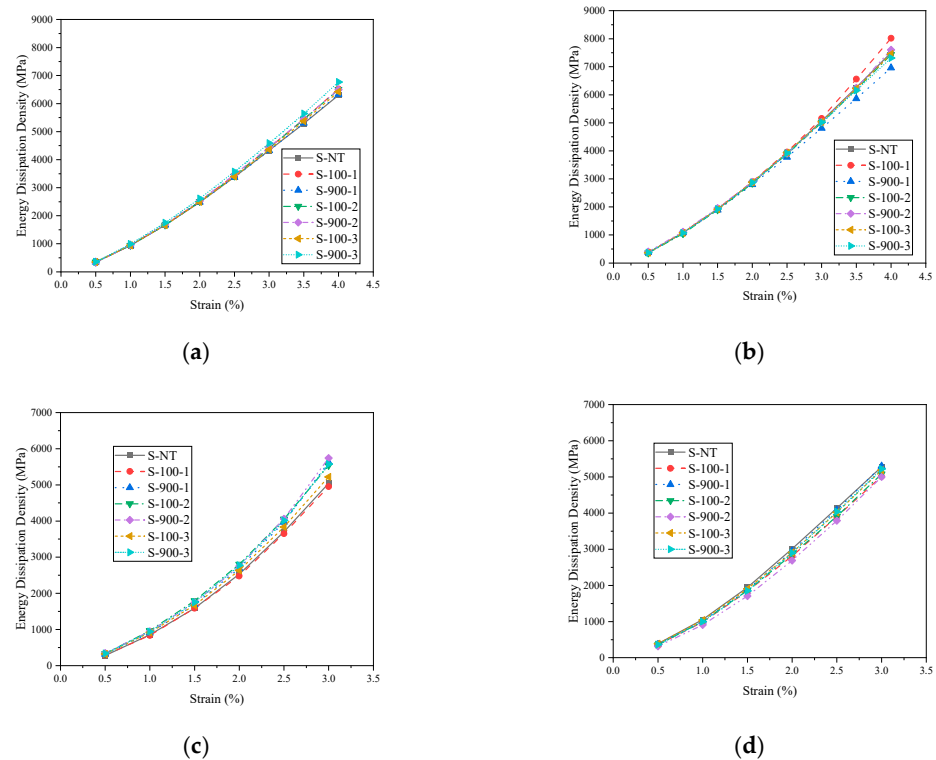


Figure 19. Energy dissipation density. (a) Q235; (b) Q345; (c) S304; (d) S316.

As shown in Figure 19a,b, for the Q235 and Q345 structural steel specimens prepared with heating-cooling treatment style 1, the energy dissipation capacity of the specimens with higher target heat temperatures was less than that of the specimens with lower target heat temperatures at the same strain level, and this difference became more obvious with an increase in strain amplitudes. This indicated that short-term heat treatment may weaken the energy dissipation capacity of Q235 and Q345 structural steels. On the contrary, for the Q235 and Q345 structural steel specimens prepared with heating-cooling treatment style 2, no obvious difference was found between the specimens with different target heat temperatures at the same strain amplitude, which meant long-term heat treatment may remove the effect of target heat temperatures on the energy dissipation capacity of Q235 and Q345 structural steels. For the Q235 and Q345 structural steel specimens prepared with heating-cooling treatment style 3, the energy dissipation capacity of the specimens with higher target heat temperatures was larger than that of the specimens with lower target heat temperatures at the same strain level owing to the hardening effect of the water cooling method. This hardening effect became more significant when the strain was beyond 1% in Q235 steel specimens, while the energy dissipation capacity of the specimens with higher target heat temperatures was once again less than that of the specimens with lower target heat temperatures at the same strain level, as seen in Q345 steel specimens when the strain was beyond 3%. This meant that the hardening effect of the water cooling method on energy dissipation was weaker than the negative effect of short-term heat treatment discussed above for the Q345 steel specimens.

As shown in Figure 19c,d, for the stainless steel specimens prepared with heating-cooling treatment style 1, the energy dissipation capacity of the specimens with higher target heat temperatures was larger than that of the specimens with lower target heat temperatures at the same strain level in both the S304 and S316 steel specimens. This difference was more obvious with an increase in strain amplitude. This meant that the short-term heat treatment effect may strengthen the energy dissipation capacity of S304 and S316 structural steels. For the specimens prepared with heating-cooling treatment style 2, there was no obvious difference in energy dissipation capacity between S304 steel

specimens with different target heat temperatures, while the energy dissipation capacity of the specimens with higher target heat temperatures was less than that of the specimens with lower target heat temperatures at the same strain level in S316 steel specimens. The reason for this phenomenon was that long-term heat treatment may eliminate the strengthening effects that elevated temperatures have on the energy dissipation capacity of S304 steel specimens and may further weaken the energy dissipation capacity of the S316 steel specimens with higher target heat temperatures. For the S304 steel specimens prepared with heating–cooling treatment style 3, the energy dissipation capacity of the specimens with higher target heat temperatures was larger than that of the specimens with lower target heat temperatures at the same strain level, and the difference was increased along with the strain amplitude because of the hardening effect of the water cooling method. In contrast, this hardening effect was insignificant in the S316 steel specimens prepared with heating–cooling treatment style 3, and no obvious difference was found in the energy dissipation capacity between the specimens with different target heat temperatures.

3.2.4. Skeleton Curve

Skeleton curves of hysteretic loops can directly reflect the mechanical properties of structural steels under cyclic loading. The Ramberg and Osgood model [31] is a commonly used constitutive relation for cyclic models, as shown in Equation (1). Therefore, the Ramberg and Osgood model was employed to fit the skeleton curves in this paper.

$$\frac{\Delta\varepsilon}{2} = \frac{\Delta\varepsilon_e}{2} + \frac{\Delta\varepsilon_p}{2} = \frac{\Delta\sigma}{2E} + \left(\frac{\Delta\sigma}{2K'}\right)^{\frac{1}{n'}} \quad (1)$$

where $\Delta\varepsilon$ is total strain amplitude, $\Delta\varepsilon_e$ is elastic strain amplitude, $\Delta\varepsilon_p$ is plastic strain amplitude, $\Delta\sigma$ is stress amplitude, E is elastic modulus, K' is cyclic enhancement coefficient, and n' is cyclic enhancement exponent.

The elastic modulus E in Equation (1) can be obtained from Figure 5a. The cyclic enhancement coefficient K' and the cyclic enhancement exponent n' can be calculated by fitting the experimental skeleton curves via the Ramberg and Osgood model, as shown in Figure 20a,b. To check the accuracy of the Ramberg and Osgood model and the proposed parameters in Figure 20, a comparison of experimental skeleton curve points and fitting curves was conducted for all the specimens in this paper. The comparison results of typical specimens are shown in Figure 21 and subfigures (a–d) show the results for the four types of structural steels, respectively (E—experimental data, F—fit curves), which showed that the imitation had good results.

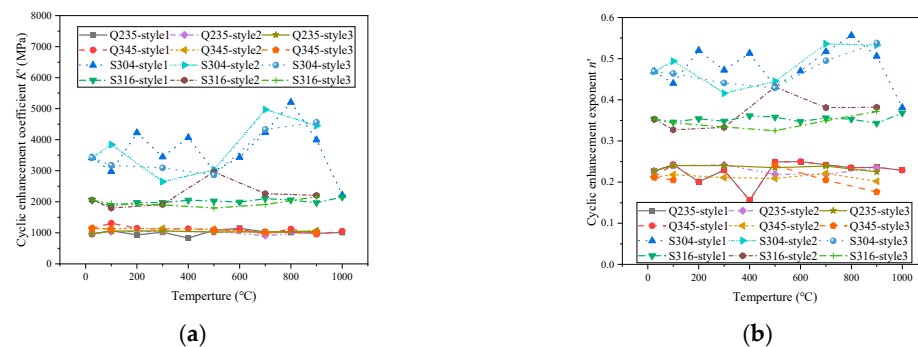


Figure 20. Parameters for Ramberg–Osgood relation. (a) Cyclic enhancement coefficient (K'); (b) Cyclic enhancement exponent (n').

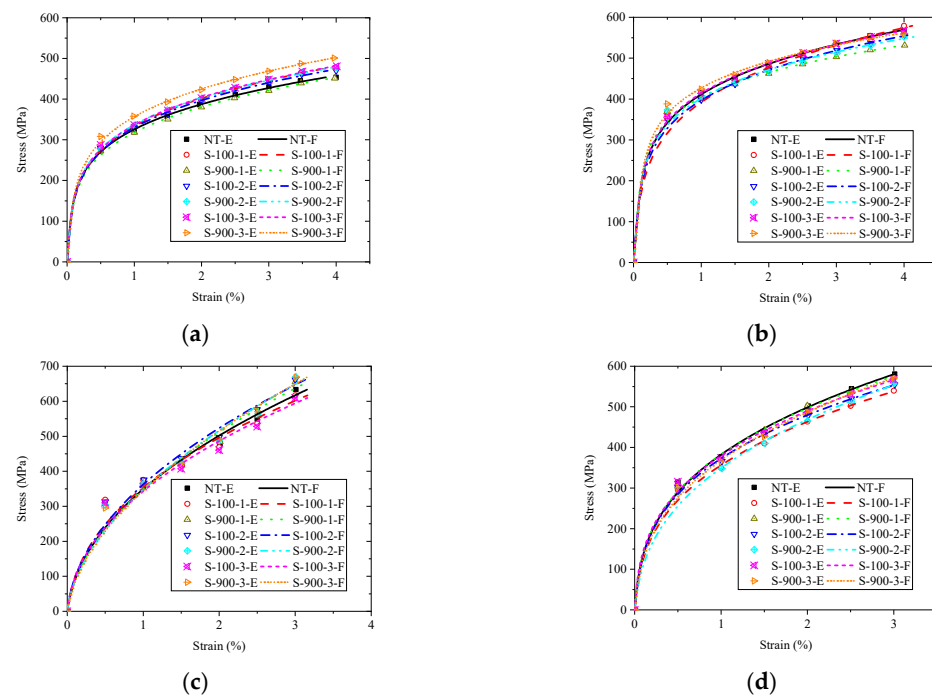


Figure 21. Comparison of experimental and fitting skeleton curves. (a) Q235; (b) Q345; (c) S304; (d) S316.

For the convenience of engineering application, a set of material parameters was proposed for Q235 and Q345 structural steels based on the data in Figures 5 and 20, as shown in Table 1. Due to the limit of the experimental data in this research, the results in Figures 5 and 20 show an obvious fluctuation, especially for S304 and S316 specimens. Therefore, the proposed values in Table 1 are rough estimates of material parameters, and it was hard to propose appropriate material parameters for S304 and S316 structural steels. More experimental data need to be collected to establish more accurate and convenient material models for Q235, Q345, S304, and S316 structural steels.

Table 1. Proposed material parameters for Q235 and Q345 structural steels.

Structural Steel	R_E	R_{fy}	K'	n'
Q235/Q345	0.95	0.9	1000	0.2

4. Conclusions

This paper experimentally investigated the cyclic performance of Chinese mild steel Grade Q235, Chinese high-strength steel Grade Q345, and Chinese stainless steel Grade S304 and S316 after exposure to various heating–cooling treatments. The main conclusions can be drawn as follows:

1. The effect of target heat temperatures, heat soak times, and cooling-down methods was negligible on the post-fire elastic moduli of Q235, Q345, and S304 structural steels, while the influence of elevated temperatures and cooling-down methods on the post-fire elastic moduli of S316 structural steels was significant.
2. The critical temperature of post-fire yielding strength was about 700 °C for all four types of structural steels, while the influences of different cooling-down methods on the residual yielding strength of the studied structural steels were insignificant in this experiment. The heating–cooling treatment styles discussed in this paper had limited effects on the ultimate strength of all four types of structural steels after cyclic loading.
3. All four types of structural steel exhibited good seismic capacity, including plump hysteretic curves and sufficient ductility, after exposure to heating–cooling treatments.

The energy dissipation capacity varied according to steel grades, target heat temperatures, heat soak times, and cooling-down methods, with the influence of steel grade on the ductility being more significant than the heating–cooling treatment styles discussed in this paper.

4. All four types of structural steels had non-Masing properties, which was unrelated to target heat temperatures, heat soak times, and cooling-down methods.
5. The Ramberg and Osgood model and corresponding model parameters can properly simulate the skeleton curves of all four types of structural steels after exposure to the heating–cooling treatments involved in this paper. Therefore, the proposed model can be applied as the constitutive relation of fire-affected steels in the post-fire seismic capacity evaluation of steel structures which are made of the four types of structural steels. However, more experimental data need to be collected to establish a more accurate and convenient material model for engineering applications.

Author Contributions: Formal analysis and writing—original draft preparation, P.D.; supervision and funding acquisition, H.L.; investigation and resources, X.X. All authors have read and agreed to the published version of the manuscript.

Funding: This research was funded by Hebei Province Science Fund for Distinguished Young Scholars, grant number E2021402006.

Institutional Review Board Statement: Not applicable.

Informed Consent Statement: Not applicable.

Data Availability Statement: Not applicable.

Conflicts of Interest: The authors declare no conflict of interest.

References

1. Lu, J.; Liu, H.; Chen, Z.; Liao, X. Experimental investigation into the post-fire mechanical properties of hot-rolled and cold-formed steels. *J. Constr. Steel Res.* **2016**, *121*, 291–310. [[CrossRef](#)]
2. Chen, Z.; Lu, J.; Liu, H.; Liao, X. Experimental study on the post-fire mechanical properties of high-strength steel tie rods. *J. Constr. Steel Res.* **2016**, *121*, 311–329. [[CrossRef](#)]
3. Qiang, X.; Bijlaard, F.S.K.; Kolstein, H. Post-fire mechanical properties of high strength structural steels S460 and S690. *Eng. Struct.* **2012**, *35*, 1–10. [[CrossRef](#)]
4. Kang, L.; Wu, B.; Liu, X.; Ge, H. Experimental study on post-fire mechanical performances of high strength steel Q460. *Adv. Struct. Eng.* **2021**, *24*, 2791–2808. [[CrossRef](#)]
5. Sajid, H.U.; Kiran, R. Post-fire mechanical behavior of ASTM A572 steels subjected to high stress triaxialities. *Eng. Struct.* **2019**, *191*, 323–342. [[CrossRef](#)]
6. Qiang, X.; Bijlaard, F.S.K.; Kolstein, H. Post-fire performance of very high strength steel S960. *J. Constr. Steel Res.* **2013**, *80*, 235–242. [[CrossRef](#)]
7. Chiew, S.P.; Zhao, M.S.; Lee, C.K. Mechanical properties of heat-treated high strength steel under fire/post-fire conditions. *J. Constr. Steel Res.* **2014**, *98*, 12–19. [[CrossRef](#)]
8. Wang, W.; Liu, T.; Liu, J. Experimental study on post-fire mechanical properties of high strength Q460 steel. *J. Constr. Steel Res.* **2015**, *114*, 100–109. [[CrossRef](#)]
9. Wang, F.; Lui, E.M. Experimental study of the post-fire mechanical properties of Q690 high strength steel. *J. Constr. Steel Res.* **2020**, *167*, 105966. [[CrossRef](#)]
10. Li, G.; Lyu, H.; Zhang, C. Post-fire mechanical properties of high strength Q690 structural steel. *J. Constr. Steel Res.* **2017**, *132*, 108–116. [[CrossRef](#)]
11. Zhou, H.; Wang, W.; Wang, K.; Xu, L. Mechanical properties deterioration of high strength steels after high temperature exposure. *Constr. Build. Mater.* **2018**, *199*, 664–675. [[CrossRef](#)]
12. Zhang, C.; Wang, R.; Song, G. Post-fire mechanical properties of Q460 and Q690 high strength steels after fire-fighting foam cooling. *Thin-Walled Struct.* **2020**, *156*, 106983. [[CrossRef](#)]
13. Gunalan, S.; Mahendran, M. Experimental investigation of post-fire mechanical properties of cold-formed steels. *Thin Wall Struct.* **2014**, *842*, 41–54. [[CrossRef](#)]
14. Wang, X.; Tao, Z.; Song, T.; Han, L. Stress-strain model of austenitic stainless steel after exposure to elevated temperatures. *J. Constr. Steel Res.* **2014**, *99*, 129–139. [[CrossRef](#)]
15. Li, X.; Lo, K.H.; Kwok, C.T.; Sun, Y.F.; Lai, K.K. Post-fire mechanical and corrosion properties of duplex stainless steel: Comparison with ordinary reinforcing-bar steel. *Constr. Build. Mater.* **2018**, *174*, 150–158. [[CrossRef](#)]

16. Huang, Y.; Young, B. Mechanical properties of lean duplex stainless steel at post-fire condition. *Thin-Walled Struct.* **2018**, *130*, 564–576. [[CrossRef](#)]
17. Smith, C.I.; Kirby, B.R.; Lapwood, D.G.; Cole, K.J.; Cunningham, A.P.; Preston, R.R. The reinstatement of fire damaged steel framed structures. *Fire Saf. J.* **1981**, *4*, 21–62. [[CrossRef](#)]
18. Wang, X.; Tao, Z.; Song, T.; Han, L. Mechanical properties of austenitic stainless steel after exposure to fire. Research and Applications in Structural Engineering, Mechanics and Computation. In Proceedings of the Fifth International Conference on Structural Engineering, Mechanics and Computation, Cape Town, South Africa, 2–4 September 2013.
19. Wang, X.; Tao, Z.; Hassan, M.K. Post-fire behaviour of high-strength quenched and tempered steel under various heating conditions. *J. Constr. Steel Res.* **2020**, *164*, 105785. [[CrossRef](#)]
20. Hai, L.; Sun, F.; Zhao, C.; Li, G.; Wang, Y. Experimental cyclic behavior and constitutive modeling of high strength structural steels. *Constr. Build. Mater.* **2018**, *189*, 1264–1285. [[CrossRef](#)]
21. Shi, Y.; Wang, M.; Wang, Y. Experimental and constitutive model study of structural steel under cyclic loading. *J. Constr. Steel Res.* **2011**, *67*, 1185–1197. [[CrossRef](#)]
22. SAC. *GB/T700-2006*; Carbon Structural Steels. China Standard Press: Beijing, China, 2006.
23. SAC. *GB/T1591-2008*; High Strength Low Alloy Structural Steels. China Standard Press: Beijing, China, 2008.
24. SAC. *GB/T1220-2007*; Stainless Steel Bars. China Standard Press: Beijing, China, 2007.
25. SAC. *GB/T3280-2015*; Cold Rolled Stainless Steel Plate, Sheet and Strip. China Standard Press: Beijing, China, 2015.
26. SAC. *GB/T15248-2008*; The Test Method for Axial Loading Constant-Amplitude Low-Cycle Fatigue of Metallic Materials. China Standard Press: Beijing, China, 2008.
27. SAC. *GB/T 22315-2008*; Metallic Material-Determination of Modulus of Elasticity and Poisson's Ratio. China Standard Press: Beijing, China, 2008.
28. Skelton, R.P.; Maier, H.J.; Christ, H.J. The Bauschinger effect, Masing model and the Ramberg–Osgood relation for cyclic deformation in metals. *Mater. Sci. Eng. A* **1997**, *238*, 377–390. [[CrossRef](#)]
29. Chen, Y.; Sun, W.; Chan, T. Effect of Loading Protocols on the Hysteresis Behaviour of Hot-Rolled Structural Steel with Yield Strength up to 420 MPa. *Adv. Struct. Eng.* **2013**, *16*, 707–719. [[CrossRef](#)]
30. Zhou, F.; Li, L. Experimental study on hysteretic behavior of structural stainless steels under cyclic loading. *J. Constr. Steel Res.* **2016**, *122*, 94–109. [[CrossRef](#)]
31. Ramberg, W.; Osgood, W.R. Description of Stress-Strain Curves by Three Parameters. *NACA Tech. Note No. 902*; 1943. Available online: <https://ntrs.nasa.gov/citations/19930081614> (accessed on 8 May 2022).